GEOPHYSICAL RESEARCH LETTERS, VOL. 22, NO. 24, PAGES 3489-3492, DECEMBER 15, 1995

Lidar observations of stratospheric ozone and aerosol above the Canadian high arctic during the 1994-95 winter

D.P. Donovan, J.C. Bird, J.A. Whiteway, T.J. Duck, S.R. Pal, and A.I. Carswell

Institute for Space and Terrestrial Science and the Department of Physics and Astronomy, York University, North York, Ontario, Canada

Abstract. This letter reports on lidar observations of arctic stratospheric ozone and aerosol made from late December 1994 to mid-March 1995. These observations were conducted at Eureka (80°N,86.42°W) in the Canadian arctic. Based on NMC potential vorticity data and aerosol observations, the lower stratosphere over Eureka was seen to be clearly within the Polar Vortex for most of the observation period. The intravortex observations showed that in the stratosphere below the 500 K potential temperature level average ozone mixing ratios decreased on the order of 15 % from early January to mid-February with an additional 15 % decrease observed from mid February to mid-March. These trends are consistent with the Upper Atmospheric Research Satellite (UARS) Microwave Limb Sounder (MLS) measurements of ozone made during the same time periods.

Introduction

Since the discovery of massive chemical depletion of ozone within the springtime Antarctic stratosphere, [*Farman et al.* 1985] there has been escalating concern over the potential for a similar scenario to develop in the Arctic. There is now ample evidence that this process first requires regions in which temperatures are low enough so that polar stratospheric clouds (PSCs) may form [*Rodriguez*, 1993]. These cloud particles then provide the surfaces for heterogeneous reactions which convert inorganic chlorine from inactive to active forms. After exposure to sunlight, these reactive chlorine compounds lead to catalytic destruction of ozone.

While evidence for chemical depletion of ozone within the arctic lower stratosphere has been reported by a number of observers [*Larsen et al.* 1994, *Manney et al.* 1994] , the decrease in ozone throughout the winter and spring has yet to approach the magnitude of an Antarctic "ozone hole". The arctic polar vortex is much more dynamically perturbed and regions with temperatures below the threshold of PSC formation are not as large or long lasting as in the Antarctic stratosphere [*Schoeberl and Hartmann*, 1991]. However, as the stratosphere is expected to cool with increasing CO_2 levels there is certainly cause for concern.

Paper number 95GL03337
0094-8534/95/95GL-03337$03.00

This letter reports on lidar observations of stratospheric ozone and aerosol that were carried out at a new observatory in the Canadian High Arctic. The observatory, operated by the Atmospheric Environment Service (AES) of Canada, is located near the permanent Canadian weather station at Eureka on Ellesmere Island (80.05 N, 86.42 W). This location is particularly interesting since its position relative to to the stratospheric polar vortex can be quite variable. The height-dependent evolution of stratospheric ozone over Eureka is presented here and discussed with regard to the changing background dynamical conditions and possible chemical depletion.

Measurement Technique

The AES/ISTS ozone Differential Absorption Lidar (DIAL) at Eureka transmits light at 308 nm (the 'on' or absorbed wavelength) and at 353 nm (the 'off' wavelength). The system parameters are similar to those given in the description by *Carswell et al.* [1993], except that the receiver has been subsequently modified to observe vibrational Raman shifted scattering from atmospheric N_2 at 332 nm (from 308 nm) and 385 nm (from 353 nm) in addition to the elastic molecular/aerosol backscatter. With respect to ozone measurements, the main advantage of observing the Raman returns is the elimination of the effect of backscattering from aerosols [*McGee et al.* 1993]. However, since the Raman backscattering cross section is relatively small, Raman DIAL ozone measurements with the Eureka system are limited to below about 22-25 km and the Rayleigh DIAL technique is used above.

Measurements of the lidar aerosol backscatter ratio, R, (the sum of the molecular and aerosol scattering divided by the molecular scattering only) measurements were made by ratioing the 353 nm elastic (molecular+aerosol) return by the 385 nm Raman return and normalizing this ratio to unity at altitudes above the aerosol layer. This method, to a large degree, removes the uncertainty associated with accounting for the aerosol extinction. Meteorological sondes launched every 12 hours provided density data used to account for molecular extinction in both the ozone and aerosol measurements. When the sondes did not reach a sufficient altitude, the lidar derived temperature profile above the aerosol layer [*Hauchecorne and Chanin*, 1980] was smoothly matched with the sonde temperature pro-

file. The sonde density profile was then extrapolated upwards on this basis.

During periods of high aerosol loading in the lower stratosphere (e.g. following Mt. Pinatubo) ozone can not accurately be measured there by DIAL systems using the 353/308nm wavelength pair [*Steinbrecht and Carswell*, 1993]. However, during the 1994/95 winter the sulfate aerosol layer was approaching background levels. Based on comparisons with the ozone values retrieved using the Raman wavelengths, the errors associated with ozone measurements made in the presence of aerosols using the Rayleigh wavelengths were found to be below a few percent under most circumstances.

As a further indication of the measurement accuracy the lidar ozone observations were compared with measurements made by ECC ozone sondes that were launched from the weather station. Figure 1 shows a comparison between sonde measurements and lidar measurements made using the Rayleigh and the Raman wavelength pairs. The data shown were derived using about 20 pairs of lidar and sonde observations. The lidar measurements used were typically averages over several hours while the sonde was launched during or within a few hours of the measurement period. The average difference between both types of lidar and EEC sonde measurements is seen to be less than about 7%. These values compare quite well with expected sonde precision and accuracy [*McDermid et al.* 1990].

Observations

Based on NMC potential vorticity (PV) maps at the 450 K potential temperature level (17–18 km) Eureka's position relative to the lower stratospheric vortex was found to vary throughout the season. In late December, Eureka was inside the vortex and remained inside until late January. During February, the vortex moved back above the Canadian Arctic and in early March Eureka was near its center for several days. As noted by Zurek et al. (submitted to Geophys. Res. Lett., 1995) the arctic polar vortex was unusually strong throughout the winter of 1994-95. Moreover temperatures below the threshold for PSC formation were unusually persistent. As shown in Figure 2 minimum vortex temperatures at 50 mbar (about 20 km or 500 K inside the vortex) were

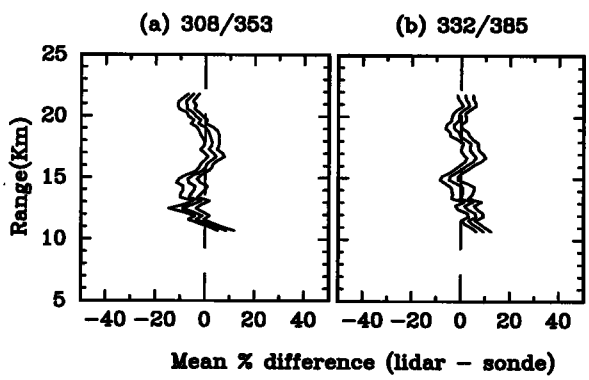

Figure 1. Average deviation between (a) O_3 concentrations measured using the 353/308 wavelength pair and EEC sondes and (b) O_3 concentrations measured using the 385/332 wavelength pair and EEC sondes. The outside lines indicate the ± standard deviation of the mean percent difference.

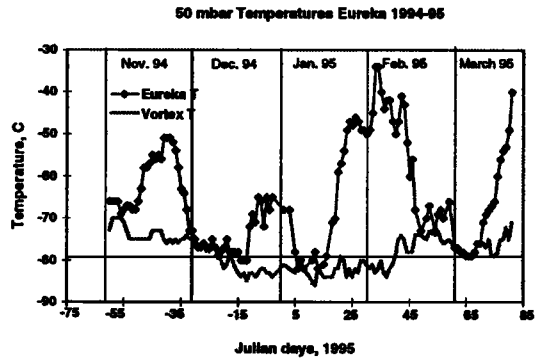

Figure 2. Vortex minimum temperature at 50 mb along with the 50 mb temperature over Eureka during the winter. The threshold for PSC formation is marked at -78°C.

below -78°C (the approximate threshold for the formation of type I PSCs) consistently between early December and February. Such conditions indicate the possibility that appreciable amounts of chemical ozone depletion could have occurred throughout the winter. Also shown in Figure 2 are the temperatures above Eureka indicating that during several time periods the coldest vortex temperatures at 50 mbar were to be found above Eureka. Indeed, during mid-December and early January PSCs were identified by the polarization sensitive Nd:YAG Lidar also at Eureka (Nagai et al., submitted to Geophys. Res. Lett., 1995).

In Figure 3 we show the the backscatter ratio (R) measured throughout the course of the winter. Here the vertical coordinate is potential temperature (θ) which is conserved during adiabatic processes. Hence, plotting against θ will remove the effects of vertical adiabatic air motions. The aerosol scattering shown here does include the aforementioned PSC events, however at 353 nm they do not significantly stand out against the background H_2SO_4/H_2O aerosol. There is a marked difference in the distribution of aerosols inside and outside of the vortex [*Browell et al.* 1993]. This is due to the fact that the large PV gradients near the vortex edge constitute a strong barrier to horizontal mixing [*Schoeberl et al.* 1992] and that diabatic descent occurs within

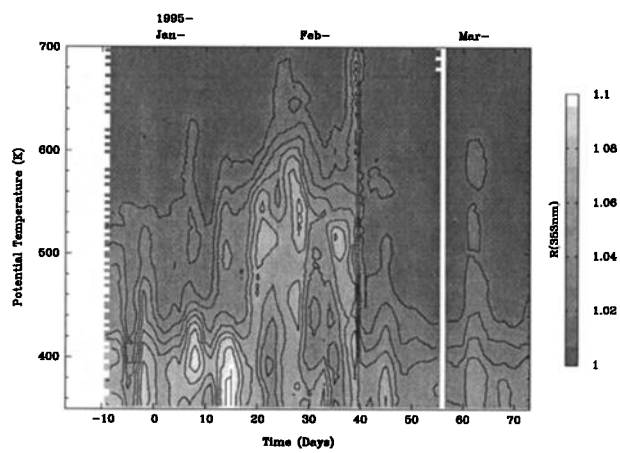

Figure 3. Scattering ratio (R) at 353 nm measured throughout the observation period. The standard deviation of the R values used in this composite were generally below 0.01 below about 22 km for a typical measurement period of 4 hours and 300 m resolution.

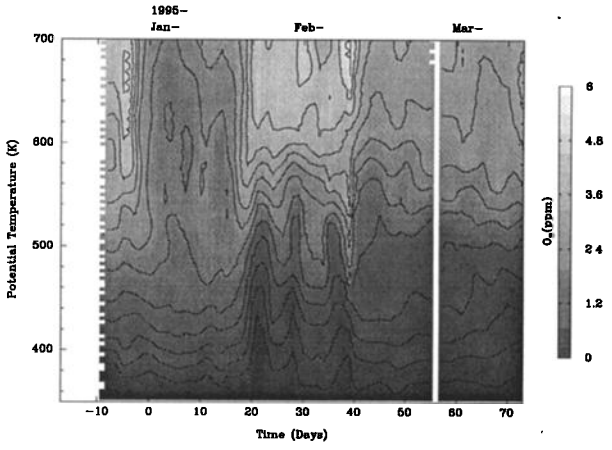

Figure 4. Ozone mixing ratio (ppmv) measured throughout the observation period.

the vortex [*Loewenstein et al.* 1990] . In general, very little aerosol resides above about 450 K (18 Km) during periods inside the vortex.

During the course of a winter, mixing ratios of atmospheric constituents will be affected by altitude dependent diabatic mean descent across potential temperature surfaces within the vortex. From Figure 3 an estimation of the average rate of diabatic descent within the vortex around the 400–450 K level can be made by noting that topmost levels of the stratospheric sulfate aerosol layer appeared to descend about 50 K between January and March. Neglecting the sedimentation velocity of the aerosol (which for aerosol with a mean radius on the order of 0.1 μm is approximately 1×10^{-3} cms^{-1}) gives an average descent rate around 0.03 cms^{-1}. This estimate of mean diabatic descent is consistent with earlier work [*Schoeberl et al.* 1992].

Since the scattering ratio behaves (to a first approximation) as a tracer and generally decreases with increasing altitude above 400 K one would expect values at a given θ level (above 400 K) to decrease throughout the winter. Ozone mixing ratio, however, generally increases with height. Thus, one would expect diabatic descent to increase ozone mixing ratios at a given θ level. In Figure 4 we show the ozone mixing ratio measured throughout the winter. Above about 550 K, the signature of diabatic descent is present. Comparison of intravortex ozone mixing ratio values near 650 K in early January with values in late February and early March seems to indicate the effects of diabatic descent on the order of 150 K (again consistent with earlier work). Below 500 K the estimated amount of diabatic descent at these levels would be expected to increase ozone mixing ratios by at least some few tenths of a ppm. However, there is no sign of the expected increase in the measured ozone mixing ratios. In fact, there is seen to be a decrease in ozone concentration indicating the possibility of the occurrence of chemical depletion.

Ozone mixing ratios measured throughout the observation season along with the PV values at various levels of potential temperature are shown in Figure 5. The values shown are averaged over ± 10 K about the level indicated. The expected correlation between PV

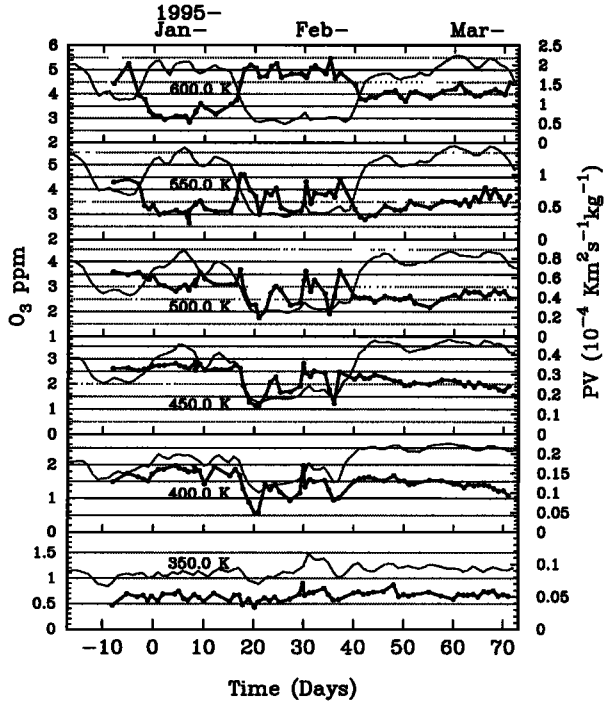

Figure 5. Ozone mixing ratio time series at different potential temperature levels (bold line). Superimposed is the NMC potential vorticity (PV) at each level.

and ozone mixing ratio (i.e. positive at lower levels and negative for higher levels [*Allaart et al.* 1993]) is evident. Also evident is the fact that over the observation period intravortex ozone concentrations above 500 K generally show an increase, whereas levels between 500 and 350 K show a notable decrease. In particular, between 500 K and 400 K a decrease of about 15 % between early January and mid February is evident with an additional 15 % decrease between mid February and early March below about 450 K. More detail can be be seen by referring to Figure 6, in which averaged intravortex ozone mixing ratio profiles in early January, late February and early March are compared.

The negative trends could be the result of chemical processes or the entrainment of mid-latitude air into the vortex. Since below about 500 K, air outside of the vortex has generally lower ozone mixing ratios than air

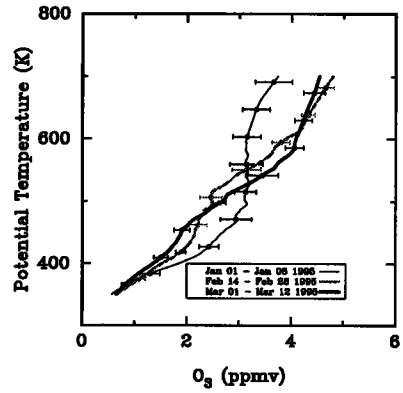

Figure 6. Intravortex average ozone mixing ratio profiles. The error bars show the standard deviation of the mean measured profiles.

inside the vortex, the entrainment of extra-vortex air at these levels would tend to decrease intravortex mixing ratios. Such entrainment of air into the vortex is more likely during periods when the vortex is disturbed [*Plumb et al.* 1994]. However, three dimensional model calculations show that, although intrusions did occur in early February, the resulting average decrease in intravortex ozone is judged to be small (*Manney et al.* submitted to Geophys. Res. Lett., 1995).

The observed decrease in ozone mixing ratio between early January and mid-February is in agreement with measurements made with the Microwave Limb Scanning instrument (MLS) on the Upper Atmospheric Research Satellite (UARS). The MLS's coverage was limited during this past winter, however, measurements did show a decrease of about 15 % in average lower stratospheric intravortex ozone (Manney et al. 1995). This value is consistent with our January-February observations over Eureka. The MLS also measured enhanced levels of ClO inside the vortex in early February which is consistent with the occurrence of chemical depletion.

The decrease in ozone mixing ratio between mid-February and March observed over Eureka is much higher than the vortex-averaged decrease measured by the MLS (15 vs. 5 %). This may be due to the fact that Eureka was, during this time period, close to the center of the vortex. Hence, the stratosphere over Eureka would have been more isolated from the effects of diabatic descent which are often greater towards the vortex edge [*Schoeberl et al.* 1992] and would be tending to increase intravortex ozone mixing ratios.

Conclusion

Lidar observations have provided a record of stratospheric aerosol and ozone throughout the winter. Ozone measurements between early January 1995, and March 1995 showed that decreases in intravortex ozone mixing ratios occurred below 500 K. These results are consistent with observations of the MLS instrument on UARS. The lidar results tend to support the claim that significant chemical depletion did occur within the arctic polar vortex during the 1994/95 winter, although, a more detailed analysis should be applied to the lidar data to more accurately separate chemical and dynamical effects.

Acknowledgments. Financial and technical support was provided by the Institute for Space and Terrestrial Science and by the Atmospheric Environment Service of Canada. The contributions of staff members from Optech Incorporated are gratefully acknowledged. We wish to thank Japanese colleagues from the Meteorological Research Institute and the Communications Research Laboratory for providing additional ozone sondes. We also wish to thank Dr. G.L. Manney at JPL who provided information regarding MLS observations as well as potential vorticity data calculated from the U.S. NMC analysis.

References

Allaart, M.A.F., H. Kelder, and L.C. Heijboer, On the relation between ozone and potential vorticity, Geophys. Res. Lett., *20*, 811-814, 1993.

Browell et al. Ozone and Aerosol Changes During the 1991-92 Airborne Arctic Stratospheric Expedition, *Sci. 261*, 1155-1158, 1993.

Carswell, A.I., A. Ulitsky, and D.I. Wardle, Lidar measurements of the Arctic stratosphere, *SPIE 2049*, 9–23, 1993.

Farman, J.C., B.G. Gardiner, and J.D. Shanklin, Large losses of total ozone in Antarctica reveal seasonal CLO_x/NO_x interaction, *Nature, 315*, 207–210, 1985.

Hauchecorne, A. and M.L. Chanin, Density and temperature profiles obtained by lidar between 35 and 70 km, Geophys. Res. Lett., *7*, 1980.

Larsen N., and B. Knudsen et al., Ozone depletion in the arctic stratosphere in early 1993, Geophys. Res. Lett.*21*, 1611–1614, 1994.

Loewenstein, M., J.R. Podolske, and K.R. Chan, N_2O as a dynamical tracer in the arctic vortex, Geophys. Res. Lett., *17*, 477–480, 1990.

Manney, G. L., et al., Chemical depletion of ozone in the Arctic lower stratosphere during winter 1992-93, *Nature, 370*, 429–434, 1994.

McDermid, I.S. et al., Comparison of ozone profiles from ground-based lidar, electrochemical concentration cell balloon sonde, ROCOZ-A rocket ozonesonde and stratospheric aerosol and gas experiment satellite measurements, J. Geophys. Res., *95*, 10,037–10,042, 1990.

McGee, T.J. et al., Raman dial measurements of stratospheric ozone in the presence of volcanic aerosols, Geophys. Res. Lett., *20*, 955–958, 1993.

Plumb, R.A., et al. Intrusions into the lower stratospheric Arctic vortex during the winter of 1991–1992, J. Geophys. Res.,*99*, 1089–1105, 1994.

Rodriguez, J.M., Probing stratospheric ozone, *Science, 261*, 1128–1129, 1993.

Schoeberl, M.R., and D.L.Hartmann, The dynamics of the stratospheric polar vortex and its relation to springtime ozone depletions *Science, 251*, 46–52, 1991.

Schoeberl, M. R., et al. The structure of the polar vortex, J. Geophys. Res., *97*, 7859–7881, 1992.

Steinbrecht W., and A.I. Carswell, Evaluation of the effects of Mount-Pinatubo aerosol on differential absorption lidar measurements of stratospheric ozone, J. Geophys. Res., *100*, 1215–1233, 1995.

Institute for Space and Terrestrial Science 4700 Keele Street, North York, ON., Canada, M3J 1P3

(received July 11, 1995; revised September 26, 1995; accepted October 3, 1995.)